

DOI: 10.24425/amm.2019.126211

D. OLESZAK^{*#}, B. KUROWSKI^{*}, T. PIKULA^{**}, M. PAWLYTA^{***}, M. SENNA^{****}, H. SUZUKI^{*****}

TOWARDS CUBIC MODIFICATION OF $\text{Li}_7\text{La}_3\text{Zr}_2\text{O}_{12}$ COMPOUND BY MECHANICAL MILLING AND ANNEALING OF POWDERS

The aim of these studies was to obtain single phase cubic modification of $\text{Li}_7\text{La}_3\text{Zr}_2\text{O}_{12}$ by mechanical milling and annealing of $\text{La}(\text{OH})_3$, Li_2CO_3 and ZrO_2 powder mixture. Fritsch P5 planetary ball mill, Rigaku MiniFlex II X-ray diffractometer, Setaram TG-DSC 1500 analyser and FEI Titan 80-300 transmission electron microscope were used for sample preparation and investigations. The applied milling and annealing parameters allowed to obtain the significant contribution of c- $\text{Li}_7\text{La}_3\text{Zr}_2\text{O}_{12}$ in the sample structure, reaching 90%. Thermal measurements revealed more complex reactions requiring further studies.

Keywords: lithium-ion batteries; solid state electrolyte; mechanical milling; XRD; DSC/TG

1. Introduction

Conventional lithium-ion liquid-electrolyte batteries are widely used in portable electronic equipment such as laptop computers, cell phones, and electric vehicles. However, they have several shortcomings, including expensive sealing agents and inherent hazards of fire and leakages. Utilization of solid state electrolytes is a way to overcome the safety issues of liquid electrolytes.

The performance of a solid state battery depends on the diffusion of ions within the electrolyte. Therefore, solid electrolytes are required to have high ionic conductivity and very low electronic conductivity and should exhibit a high degree of chemical stability [1]. Crystalline materials such as lithium halides, lithium nitride, oxy-salts, and sulphides have been found to be good as solid electrolytes. The most favourable features of the solid electrolyte are that there is no corrosive or explosive leakage and the chance of internal short circuit is limited, all resulting in safety increasing [2].

Different types of solid state electrolytes have been employed, based on their configurations and electrode/electrolyte materials setups. Therefore, solid state electrolytes are broadly classified into two types, thin film solid state electrolytes and bulk solid state electrolytes, which are usually prepared by conventional solid state route, i.e. cold compaction of the powders and their sintering. Sometimes additional annealing or heat treatment is applied.

Solid state electrolytes with the garnet structure are used frequently [3] and Li-containing garnet-type oxides are consid-

ered as the most promising fast ion-conducting electrolytes for solid state lithium-ion batteries. Especially cubic $\text{Li}_7\text{La}_3\text{Zr}_2\text{O}_{12}$ (c-LLZO) is regarded as a good candidate for this application. However, the traditional manufacturing technique, including powder compaction and sintering, is energy – and time – consuming, because typical processing temperature and time are 1200°C and 36 h, respectively. Additionally, loss of lithium, the appearance of tetragonal modification of LLZO in the structure and the formation of harmful, undesired side phases after sintering is frequently observed. Therefore, application of mechanical milling of precursor powders prior to their compaction can enhance the powders reactivity and can result in easier formation of c-LLZO.

The aim of this work was to study the possibility of c-LLZO phase formation by mechanical milling followed by powders annealing, applying selected processing parameters and to characterize structurally the obtained materials.

2. Experimental

For the mechanosynthesis of LLZO the powders of ZrO_2 (Tosoh, purity 99.9%), $\text{La}(\text{OH})_3$ (Aldrich, 99.9%) and Li_2CO_3 (Aldrich, 99.8%) were used. The size of all powders was sub-micrometric. The powders were mixed in the molar ratio 7:3:2 corresponding to the formation of $\text{Li}_7\text{La}_3\text{Zr}_2\text{O}_{12}$. The milling processes were performed in a Fritsch P5 planetary ball mill at 250 rotations per minute for various milling times. Alumina container and alumina balls with 8 mm diameter were used. The

* WARSAW UNIVERSITY OF TECHNOLOGY, FACULTY OF MATERIALS SCIENCE AND ENGINEERING, 141 WOLOSKA STR., 02-507 WARSAW, POLAND

** LUBLIN UNIVERSITY OF TECHNOLOGY, FACULTY OF ELECTRONICS AND INFORMATION TECHNOLOGY, 38A NADBYSTRZYCKA STR., 20-618 LUBLIN, POLAND

*** SILESIA UNIVERSITY OF TECHNOLOGY, INSTITUTE OF ENGINEERING MATERIALS AND BIOMATERIALS, 18A KONARSKIEGO STR., 44-100 GLIWICE, POLAND

**** KEIO UNIVERSITY, FACULTY OF SCIENCE AND TECHNOLOGY, YOKOHAMA, JAPAN

***** SHIZUOKA UNIVERSITY, RESEARCH INSTITUTE OF ELECTRONICS, HAMAMATSU, JAPAN

Corresponding author: dariusz.oleszak@pw.edu.pl

ball-to-powder weight ratio was 45:1. The milling processes were performed in air and no process control agent was added. After milling the powders were subjected to annealing in a furnace in air at 750°C for 3 h.

The phase composition of the powders subjected to milling and annealing was examined by X-ray diffraction using Rigaku MiniFlex II diffractometer equipped with CuK α radiation ($\lambda = 0.15418$ nm). Detailed analysis of the obtained diffractograms was performed by HighScore Plus computer program. Rietveld method was applied for refinement of the crystalline structure [4]. Thermal measurements were performed using Setaram TG-DSC 1500 analyser in the temperature range 50-1100°C. The powders were placed in a Pt container and heated at heating rate of 10°Cmin⁻¹ in argon atmosphere.

For TEM studies specimens were prepared by dispersing a small amount of the sample in methanol and putting a droplet of the suspension on a microscope copper grid covered with carbon. TEM investigations were undertaken with a field-emission transmission electron microscope (FEI Titan 80-300 TEM/STEM) with a super twin lens operated at 300 kV and equipped with an annular dark-field detector. The chemical composition was determined in the same apparatus using energy dispersive spectroscopy (EDS).

3. Results and discussion

Fig. 1a shows the XRD pattern of the initial powder mixture. The diffraction lines belonging to the starting components of La(OH)₃, Li₂CO₃ and ZrO₂ can be found. Despite the fact that the powders were in submicrometric range, the diffraction lines are not broadened significantly. Contrary, the XRD pattern recorded for the powders subjected to mechanical milling for 10 h reveals a significant broadening of the registered diffraction lines (Fig. 1b).

The pattern is dominated by lanthanum hydroxide peaks, however the lines belonging to other starting phases still exist. The calculated by Scherrer's formula crystallite size of La(OH)₃ was 50 nm \pm 10 nm. Thus, the milling process continued up to

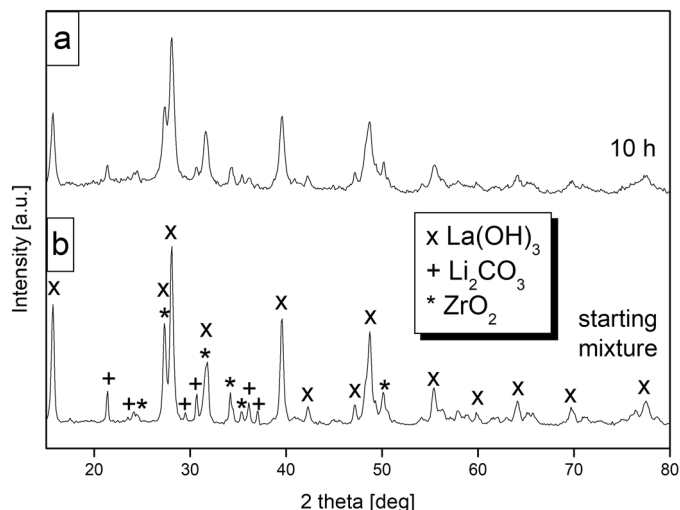


Fig. 1. XRD patterns of the starting powder mixture before milling (a) and after 10 h of milling (b)

10 h does not result in phase composition changes. The broadening of the registered XRD lines testifies the crystallite size refinement only.

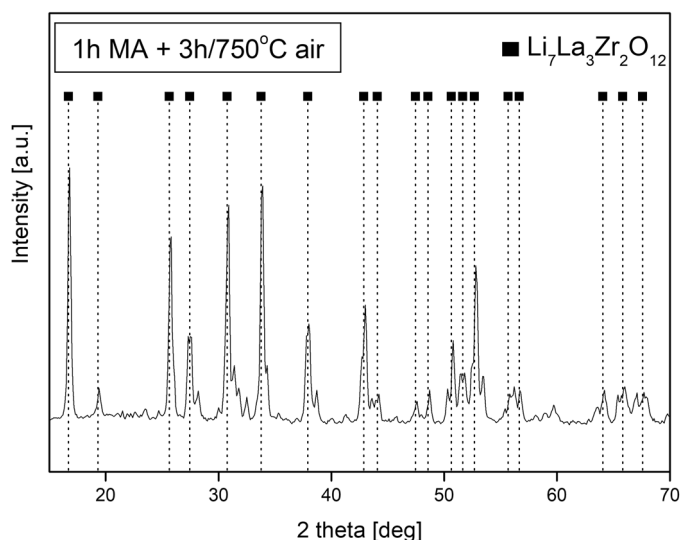


Fig. 2. XRD pattern of the sample annealed in air at 750°C for 3 h

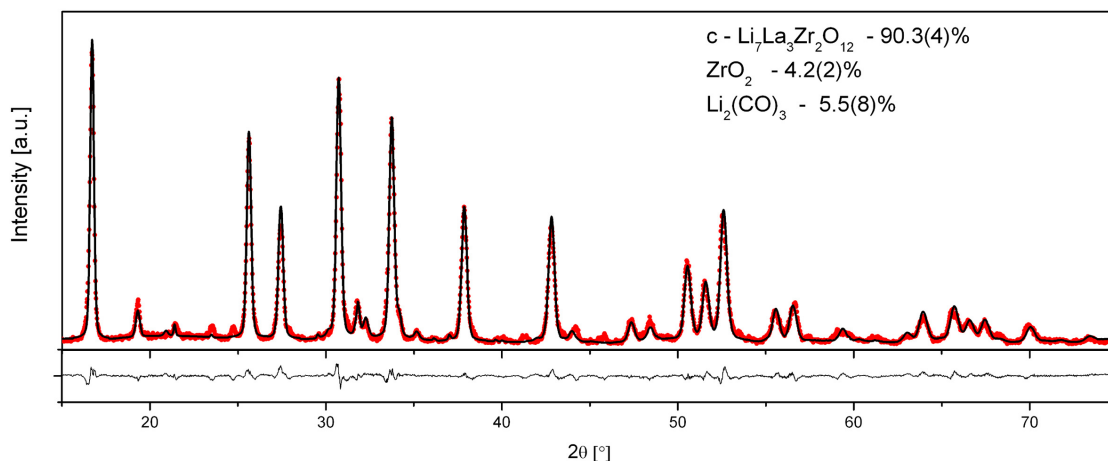


Fig. 3. Rietveld analysis for the sample annealed in air at 750°C for 3 h

Next, the annealing of the powders in air at 750°C for 3 h was performed and from Fig. 2 it can be recognized that a new compound was formed. Detailed analysis shows that majority of recorded diffraction lines are identified as belonging to cubic modification of $\text{Li}_7\text{La}_3\text{Zr}_2\text{O}_{12}$ (PDF4+ card no 01-080-9103). In order to calculate the contribution of $c\text{-Li}_7\text{La}_3\text{Zr}_2\text{O}_{12}$ and to identify other phases, Rietveld analysis was performed (Fig. 3). It was found that the contribution of $c\text{-Li}_7\text{La}_3\text{Zr}_2\text{O}_{12}$ in the structure reaches 90.3 wt. %. Remaining phases were identified as unreacted Li_2CO_3 (5.5 %) and ZrO_2 (4.2 %).

Assuming Ia-3d space group for $c\text{-Li}_7\text{La}_3\text{Zr}_2\text{O}_{12}$ the best numerical fit of the diffractogram was achieved. The lattice parameter was calculated as $a = 13.025 \text{ \AA}$ and it agrees well with the data reported for $c\text{-Li}_7\text{La}_3\text{Zr}_2\text{O}_{12}$ prepared by co-precipitation method [5]. The values of fitting parameters usually used for the estimation of fitting quality ($\chi^2 = 2.5$, $R_{\text{exp}} = 4.2$, $R_{\text{prof}} = 6.8$, $R_{\text{w prof}} = 9.6$) testify good quality of the obtained results.

Thermal analysis of the milled and annealed powders reveals three exothermic effects at the DSC curve, accompanied by sample mass changes (Fig. 4).

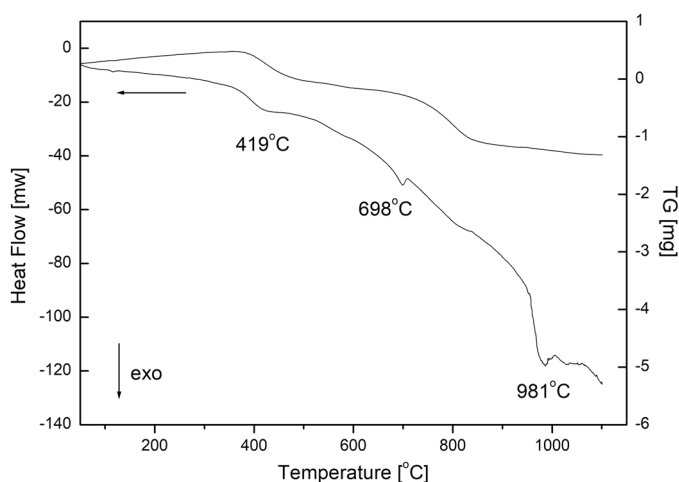


Fig. 4. DSC/TG curves for the sample annealed in air at 750°C for 3 h

The heat effect around 419°C can be related to the decomposition of $\text{La}(\text{OH})_3$ and formation of La_2O_3 [6]. On the other hand, the effect around 698°C can be assigned to the decomposition of Li_2CO_3 [7], while high temperature transformation at 981°C can correspond to the cubic-tetragonal transition of LLZO [8]. The results of DSC/TG measurements are in agreement with the results of Rietveld analysis regarding the possible decomposition of residual Li_2CO_3 during heating the powders. However, the first exothermic peak at the DSC curve was assigned to the decomposition of $\text{La}(\text{OH})_3$, which presence was not confirmed by Rietveld analysis. On the other hand, the decomposition of Li_2CO_3 accompanied by the evolution of CO_2 can take place also at lower temperature [9]. As a result, the sequence of chemical reactions can be more complex, including the decomposition of $\text{La}(\text{OH})_3$ into LaOOH and H_2O , followed by the reaction with CO_2 and formation of $\text{La}_2\text{O}_2\text{CO}_3$ which decomposes into La_2O_3 and again CO_2 [6]. Therefore, the possible presence of La_2O_3

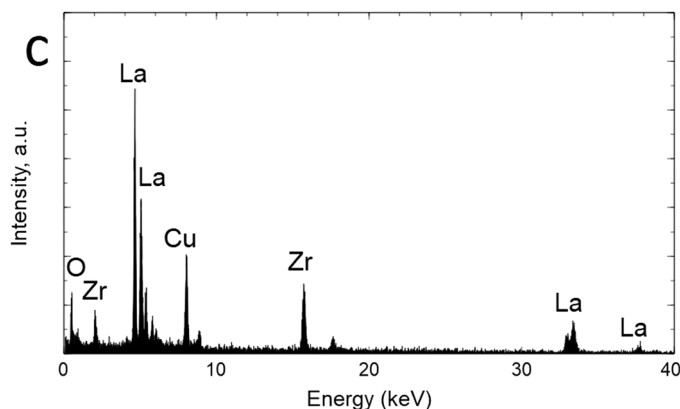
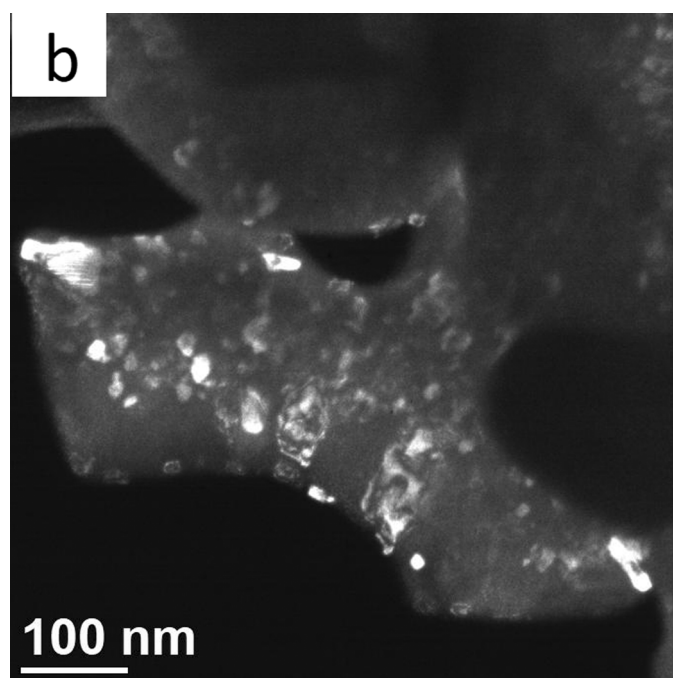
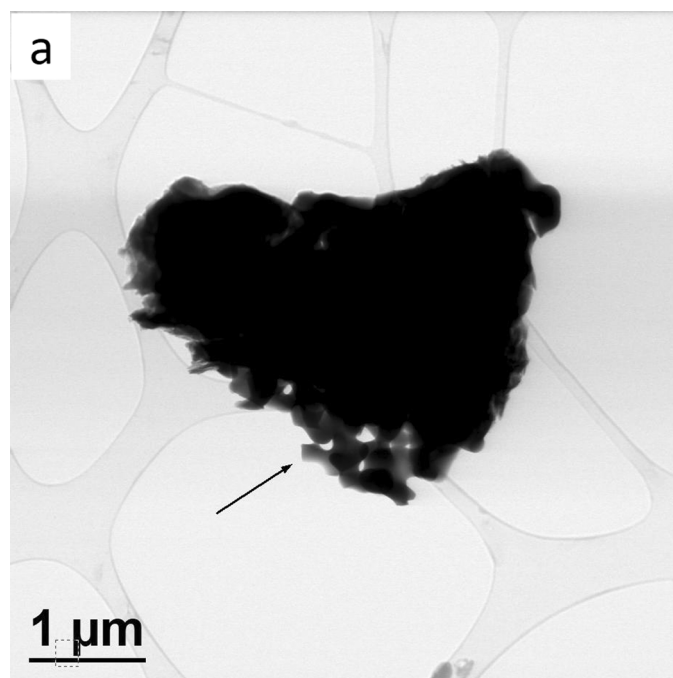


Fig. 5. BF TEM image of the synthesised powder particle (a); DF TEM image of part indicated by an arrow in Fig. 5a (b); the result of EDS analysis for corresponded area (c)

needs a confirmation by XRD studies of the sample after DSC measurement.

For further characterization of the synthesised powders TEM studies were performed. Fig. 5 a shows the morphology of an exemplary grain. Powder particle with a size of approximately 3 micrometres is of an irregular shape. A DF TEM image obtained for a part indicated by an arrow on previous figure confirms the nanocrystalline nature of the powder (Fig. 5 b). The EDS analysis confirmed the presence of La, Zr and O (Fig. 5 c). The presence of Cu is ambiguous. In that case, EDS results should be treated very carefully because it may be an effect of characteristic X-rays generated in the copper elements of a microscope.

4. Conclusions

An attempt has been undertaken to apply mechanical milling of the powder mixture of $\text{La}(\text{OH})_3$, Li_2CO_3 and ZrO_2 in appropriate proportions, followed by powders annealing, to obtain single phase, cubic modification of $\text{Li}_7\text{La}_3\text{Zr}_2\text{O}_{12}$. The obtained results indicate that milling process results in the refinement of the powders microstructure only and no phase transformations are observed. The applied annealing parameters allowed to obtain the significant contribution of $\text{c-Li}_7\text{La}_3\text{Zr}_2\text{O}_{12}$ in the sample structure, reaching 90 %. However, unreacted lithium carbonate and zirconia were also detected. The DSC curve recorded for the milled and annealed powders suggests, besides decomposition of Li_2CO_3 , more complex reactions requiring further studies.

Acknowledgements

Financial support from the National Centre for Research and Development in the framework of V4-Japan joint research project "AdOX" under the contract no V4-Jap/4/2016 is highly appreciated.

REFERENCES

- [1] V. Thangadurai, *Ionics* **12**, 81-92 (2006).
- [2] N.A. Anurova, V.A. Blatov, G.D. Ilyushin, O.A. Blatova, A.K. Ivanov-Schitz, L.N. Demyanets, *Solid State Ionics* **179**, 2248-2254 (2008).
- [3] S. Teng, J. Tan, A. Tiwari, *Curr. Opin. Solid State Mater. Sci.* **18**, 29-38 (2014).
- [4] H.M. Rietveld, *J. Appl. Cryst.* **2**, 65-71 (1969).
- [5] H. Xie, J.A. Alonso, Y. Li, M.T. Fernández-Díaz, J.B. Goodenough, *Chem. Mater.* **23**, 3587-3589 (2011).
- [6] G. Hongxia, Ch. Kai, Y. Di, M. Ao, H. Mian, L. Yuanhua, N. Cewen, *Rare Metal Materials and Engineering* **45** (3), 612-616 (2016).
- [7] E. Yi, W. Wang, J. Kieffer, R.M. Laine, *Journal of Power Sources* **352**, 156-164 (2017).
- [8] X.P. Wang, Y. Xia, J. Hu, Y.P. Xia, Z. Zhuang, L.J. Guo, H. Lu, T. Zhang, Q.F. Fang, *Solid State Ionics* **253**, 137-142 (2013).
- [9] I. Quinzeni, D. Capsoni, V. Berbenni, P.O. Mustarelli, M. Sturini, M. Bini, *Materials Chemistry and Physics* **185**, 55-64 (2017).